

---

# Decentralized agent-based modeling

---

Anonymous Author(s)

Affiliation

Address

email

## Abstract

1 The utility of agent-based models for practical decision making depends upon their  
2 ability to recreate populations with great detail and integrate real-world data streams.  
3 However, incorporating this data can be challenging due to privacy concerns. We  
4 alleviate this issue by introducing a paradigm for secure agent-based modeling.  
5 In particular, we leverage secure multi-party computation to enable decentralized  
6 agent-based simulation, calibration, and analysis. We believe this is a critical step  
7 towards making agent-based models scalable to the real-world application.

## 8 1 Introduction

9 Agent-based modeling (ABMing) is a bottom-up simulation technique wherein a system is modeled  
10 through the interaction of autonomous decision-making entities referred to as agents. Due to their  
11 granular approach, ABMs are a promising tool for real-world decision-making and policy design  
12 and constitute an active field of research across economics [5, 12, 33], biology [44, 27], and  
13 epidemiology [6, 52, 35, 32]. Wider adoption of ABMs, however, is hindered by (1) the need  
14 for microdata to generate the underlying agent population, and (2) the often large computational  
15 resources required to run, calibrate, and analyze an ABM. Recently, there has been significant  
16 progress towards developing new design patterns for ABMs, which exploit tensorization [18, 17]  
17 and differentiability [19, 3] of simulators. This has alleviated the computational burdens associated  
18 with ABM simulation [18], calibration [19, 49], and analysis [48] by granting access to modern  
19 computational techniques such as GPU computing and differentiable programming, allowing ABMs  
20 to scale to populations comprised of millions of agents [51, 10].

21 Yet, the increase in computational efficiency for ABMs can be inconsequential if the quality of the  
22 underlying population microdata is poor. Currently, prevalent approaches involve the construction  
23 of synthetic populations designed to align with a predefined set of summary statistics derived from  
24 real-world observations. For instance, in epidemiological ABMs, the population is crafted to replicate  
25 summary statistics obtained from census data [45, 13, 6, 15, 46]. However, it is essential to recognize  
26 that the limited granularity of census data arises primarily from privacy considerations rather than  
27 actual scarcity of available data. As ABMs continue to scale towards one-to-one representations  
28 of real-world systems, there remains a fundamental limitation in their modeling potential as long  
29 as privacy are not in place. Previous attempts to augment ABM data with additional information,  
30 such as mobility or health data, have resulted in data leaks that exposed agents' personal information  
31 [1, 34, 21]. These incidents underscore the need for a decentralized approach to ABMing, where  
32 each agent's sensitive information is kept confidential throughout the modeling process.

33 Motivated by this, we introduce a new paradigm for agent-based simulation that ensures the confiden-  
34 tiality of each agent's sensitive information. Leveraging techniques drawn from secure multi-party  
35 computation [38], we develop privacy-preserving protocols for the simulation, calibration, and analy-  
36 sis of ABMs. These protocols offer robust security guarantees to agents while preserving the ability  
37 of ABMs to effectively model complex systems. Moreover, our methodology enables secure ABMs to

38 take advantage of differentiable programming, allowing them to be integrated into machine learning  
 39 pipelines, further boosting their modeling capabilities.

40 In summary, this work constitutes to our knowledge the first protocol for privacy-preserving ABMs  
 41 that enables their simulation and calibration. We hope that this development will pave the way for the  
 42 secure and practical utilization of ABMs as valuable tools for policy-making in real-world settings.

## 43 2 Agent-based models

44 Consider an ABM with  $N$  agents  $A = \{1, 2, \dots, N\}$ . We denote by  $\mathbf{z}_i(t)$  the state of agent  $i$  at time  
 45  $t$  which encapsulates both fixed and time-evolving properties of the simulation agents. For instance,  $\mathbf{z}$   
 46 can represent age and disease status of human agents in epidemiological models; and account balance  
 47 of firms in a financial auction model. As the simulation proceeds, an agent  $i$  updates their state  $\mathbf{z}_i(t)$   
 48 by interacting with their neighbors  $\mathcal{N}_i(t)$  and the environment  $\mathcal{E}(t)$ . We assume that the interaction  
 49 of agents with their neighbors can be conceived as message passing on a graph  $\mathcal{G} = (V, E)$ , where  
 50 the vertices  $V$  of the graph correspond to the agents, the edges  $e_{ij} \in E$  connect neighboring agents,  
 51 and interactions are represented as messages  $M_{ij}(t) = M(\mathbf{z}_i(t), \mathbf{z}_j(t), e_{ij}(t), \boldsymbol{\theta}, t)$ , where  $\boldsymbol{\theta}$  are  
 52 the ABM structural parameters. This is indeed the case for contagion models [22], for example,  
 53  $M_{ij}(t)$  may represent the transmission of infection from agent  $j$  to agent  $i$ , which may depend on the  
 54 susceptibility of agent  $i$  ( $\mathbf{z}_i$ ), the infectivity of  $j$  ( $\mathbf{z}_j$ ), the properties of the virus ( $\boldsymbol{\theta}$ ), and the nature of  
 55 the interaction ( $e_{ij}$ ). Thus, at each step  $t$ , each agent updates its state following

$$\mathbf{z}_i(t+1) = f \left( \mathbf{z}_i(t), \bigoplus_{j \in \mathcal{N}_i(t)} M_{ij}(t), \boldsymbol{\theta} \right), \quad (1)$$

56 where  $\bigoplus$  denotes an aggregation function over all received messages. The specific form of  $f$  can be  
 57 tailored to capture the unique dynamics of the system under investigation, for instance, the diversity  
 58 of contagion models can be encapsulated by different functional forms of  $f$  [22].

59 During the simulation of an ABM, a central agent (the modeler) collects a time-series of aggregate  
 60 statistics over agent states,  $\mathbf{x}_t = h(\{\mathbf{z}_i(t) \mid i \in A\})$ , which can be used to compare the output of the  
 61 model to ground-truth data. For instance, in epidemiological ABMs,  $h$  may correspond to counting  
 62 the number of infected agents, so that  $\{\mathbf{x}_t\}_t$  is a time-series of daily infections.

63 As we can see, both Equation (1) and the collection of the summary statistics require agents to  
 64 communicate their state to other agents. In following sections we introduce a methodology to perform  
 65 these operations in a privacy-preserving manner.

## 66 3 Characterizing Privacy

### 67 3.1 Threat Model

68 We assume an honest-but-curious (a.k.a semi-honest) attacker [31] which aims to learn private  
 69 information about participating agents. This private information is included in an agent’s state  $\mathbf{z}_j(t)$ ,  
 70 interaction trace  $\{\mathcal{N}_i(t) \mid \forall t\}$ , and neighborhood messages  $\{M_{ij}(t) \mid i \in A, j \in \mathcal{N}(i)\}$ . For  
 71 instance, in epidemiological models, this can correspond to the health and demographic traits, and  
 72 mobility patterns of individual agents. Such attacker can manifest as the coordinating server which  
 73 wants to surveil agents using the mobility trace or a (sub-group) of adversarial agents which may  
 74 be incentivized to steal personal health information of agent cohorts. In the context of agent-based  
 75 modeling, this information can be leaked during message passing over per-step neighborhoods  
 76 (Equation (1)) and during the collection of summary statistics over the population. The goal of this  
 77 work is to alleviate such challenges and design a privacy-preserving mechanism which can compute  
 78 functions over agents’ states without revealing private information.

### 79 3.2 Secure Multi-party Computation

80 Secure multi-party computation enables a set of agents to interact and compute a joint function of  
 81 their private inputs while revealing nothing but the output [38]. MPC protocols are coordinated with a  
 82 server (MPC server) and are designed to protect against malicious behavior of adversarial participants.

83 These malicious participants, either an agent or the server, aim to learn private information (of other  
84 entities) or cause the result of computation to be incorrect. The idea was first introduced by Yao for  
85 the two-party case [57] and generalized to multiparty settings by Goldreich, Micali and Wigderson  
86 (GMW) [26]. Among other properties, GMW protocols guarantee 1) *privacy*: so that no entity can  
87 learn anything more than its prescribed output and, 2) *correctness*: so that each agent receives the  
88 correct output. For instance, in an epidemiological ABM, this would ensure both that the personal  
89 disease status of agents is not leaked and also no agent can misrepresent their disease status. We  
90 formalize the GMW protocol and provide an intuitive example in the Appendix.

## 91 4 Private Simulation of Agent-based Models

92 First, we present the SECURESUM protocol, which enables the computation of the sum of agents  
93 inputs in a private way, based on the GMW protocol (see Subsection 6.1 for a detailed description  
94 and an example) in Algorithm 1.

---

### Algorithm 1: SECURESUM

---

**Data:** Agents  $\{1, \dots, N\}$  with secret inputs  $s_1, \dots, s_n$ , integer  $n > \max\{s_1, \dots, s_n\}$ .

**Result:** The sum of all shares  $S = s_1 + \dots + s_n$ .

1 **Splitting secret into shares and distributing:**

2 Each party  $i$  generates  $N$  shares  $s_{i1}, \dots, s_{iN} \in \mathbb{Z}_n$  which sum up to  $s_i$ .

3 Each party  $i$  distributes all their shares  $s_{i1}, \dots, s_{iN} \in \mathbb{Z}_n$  to  $1, \dots, N$ , including themselves.

4 **Secure Computation (Addition):**

5 To add the inputs securely, parties simply add their respective shares  $\sigma_i = s_{1i} + \dots + s_{Ni} \pmod n$ .

6 **Reconstruction:**

7 To reveal the final result of the computation, parties collaborate by summing their shares:

8  $S = (\sigma_1 + \sigma_2 + \dots + \sigma_n) \pmod n$ .

---

95 This protocol enables the simulation of ABMs for the case where  $\oplus$  corresponds to addition in  
96 Equation (1), which is indeed the case in all contagion models. Furthermore, as long as the agent's  
97 update function  $f$  is differentiable respect to the structural parameters  $\theta$ , which is indeed the case for  
98 many ABMs [19], each agent can store  $\nabla_{\theta} f$  for use during the calibration step. With all this in mind,  
99 we present in Algorithm 2, a privacy-preserving protocol for updating the agent's states.

---

### Algorithm 2: SECUREAGENTUPDATE

---

**Data:** Agent  $i$  with state  $\mathbf{z}_i(t)$ , Neighboring agent's messages  $\{M_{ij}(t) \mid j \in \mathcal{N}(i)\}$ , Integer  $n$ ,  
State update rule  $f$ , ABM parameters  $\theta$

**Result:** New state  $\mathbf{z}_i(t+1)$

1 Agent  $i$  calls the SECURESUM protocol with neighbors  $\{j \mid j \in \mathcal{N}(i)\}$  and integer  $n$  to get the  
sum  $M_i(t) = \sum_{j \in \mathcal{N}(i)} M_{ij}(t)$ .

2 Agent  $i$  updates its state  $\mathbf{z}_i(t+1) = f(\mathbf{z}_i(t), M_i(t), \theta)$  and stores the gradient  $\nabla_{\theta} f$ .

---

100 It is worth noting that, in contrast to general applications of the GMW protocol, only the agent who  
101 starts the protocol receives the result of the computation, since there is no need for the neighboring  
102 agents to have access to that information.

103 Next, we introduce the SECURESIMULATION protocol in Algorithm 3, where, in addition to perform-  
104 ing agent updates, we collect a time-series of aggregate statistics over the agent's population and its  
105 gradient respect to the ABM structural parameters  $\theta$ .

### 106 4.1 Private calibration of ABMs

107 Calibration refers to the process of tuning the set of structural parameters  $\theta$  so that ABM outputs  $\mathbf{x}$   
108 are compatible with given observational data  $\mathbf{y}$ . In epidemiological ABMs, for instance, this entails  
109 determining values for parameters like the reproduction number  $R_0$  and mortality rates to align with  
110 the observed daily infection or mortality data. During the calibration of an ABM, the modeler (central  
111 MPC server) requires the ability to evaluate the ABM at different values of  $\theta$ , and, in the case of

---

**Algorithm 3: SECURESIMULATION**

---

**Data:** MPC server  $C$ , Agents  $\{1, \dots, N\}$  with states  $\{z_1, \dots, z_N\}$ , ABM parameters  $\theta$ , State update rule  $f$ , Number of time-steps  $T$

**Result:** Aggregate statistics  $\mathbf{x} = x_1, \dots, x_T$  and gradients  $\nabla_{\theta}\mathbf{x}$ .

- 1  $C$  generates a large enough prime number  $P$  and the requested statistics collecting function  $h$ ; and sends them to all agents along ABM parameters  $\theta$ .
  - 2 **for**  $t = 1, \dots, T$  **do**
  - 3     **for**  $i = 1, \dots, N$  **do**
  - 4         Agent  $i$  calls the SECUREAGENTUPDATE protocol (Algorithm 2) to compute  $z_i(t + 1)$ .
  - 5         Agent  $i$  gathers its information of interest  $h(z_i(t + 1))$  and gradient  $\nabla_{\theta}h(z_i(t + 1))$ .
  - 6      $C$  calls the SECURESUM protocol with all agents to collect the aggregate statistics  $x_t$  and their gradients  $\nabla_{\theta}x_t$ .
  - 7  $C$  returns the accumulated  $\mathbf{x}$  and  $\nabla_{\theta}\mathbf{x}$ .
- 

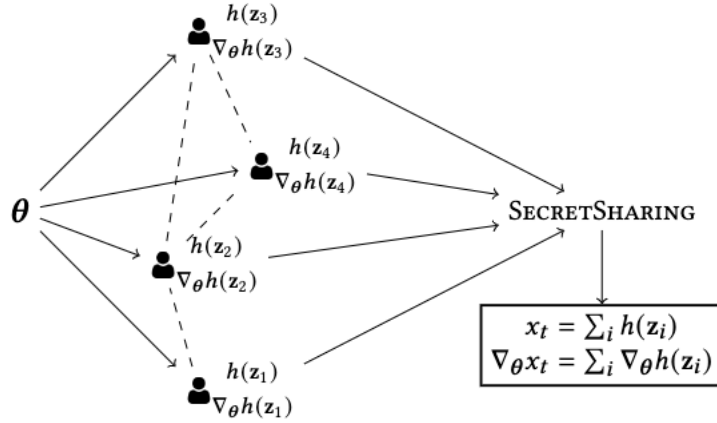


Figure 1: Diagram illustrating the SECURESIMULATION protocol for ABM parameters  $\theta$

112 gradient-assisted calibration, the gradient of the outputs with respect to  $\theta$ . These values are stored at  
113 the MPC server where they are used as part of a ML pipeline to perform calibration. The retrieval of  
114 these quantities is seamlessly enabled by the SECURESIMULATION algorithm and so all the standard  
115 calibration techniques for ABM (see, e.g., [23, 47] can be easily adapted to this private framework  
116 to ensure a decentralized calibration process that respects agent’s privacy. Moreover, the ability to  
117 retrieve the gradient in a private way enables the use of more advanced gradient-assisted techniques  
118 such as generalized variational inference [49].

## 119 5 Conclusion

120 In this paper, we have introduced a new paradigm of decentralized agent-based modeling which  
121 enables simulation and calibration on real world data, all without compromising the privacy of the  
122 agents involved. Our approach leverages MPC techniques to develop robust privacy-preserving  
123 protocols, without compromising the correctness of the ABM output. Our paradigm may be readily  
124 integrated into established platforms such as contact-tracing mobile applications, as a means to greatly  
125 improving analysis and forecasting of complex systems across diverse domains. Further, we validate  
126 by scalability of our simulation and calibration protocols via a decentralized epidemiological ABM,  
127 in the appendix.

## 128 References

- 129 [1] 2021. Indonesia Probes Suspected Data Breach on COVID-19 App. *Reuters* (Aug. 2021).

- 130 [2] Philipp Andelfinger. 2021. Differentiable Agent-Based Simulation for Gradient-  
131 Guided Simulation-Based Optimization. *arXiv:2103.12476 [cs, eess]* (March 2021).  
132 [arXiv:2103.12476 \[cs, eess\]](https://arxiv.org/abs/2103.12476)
- 133 [3] Gaurav Arya, Moritz Schauer, Frank Schäfer, and Chris Rackauckas. 2022. Automatic Differ-  
134 entiation of Programs with Discrete Randomness. *arXiv:2210.08572 [cs, math]*
- 135 [4] Samuel A. Assefa, Danial Dervovic, Mahmoud Mahfouz, Robert E. Tillman, Prashant Reddy,  
136 and Manuela Veloso. 2021. Generating Synthetic Data in Finance: Opportunities, Challenges  
137 and Pitfalls. In *Proceedings of the First ACM International Conference on AI in Finance*  
138 *(ICAIF '20)*. Association for Computing Machinery, New York, NY, USA, 1–8. <https://doi.org/10.1145/3383455.3422554>  
139
- 140 [5] Robert L. Axtell and J. Doyne Farmer. [n.d.]. Agent-Based Modeling in Economics and Finance:  
141 Past, Present, and Future. *Journal of Economic Literature* ([n. d.]). [https://doi.org/10.](https://doi.org/10.1257/jel.20221319)  
142 [1257/jel.20221319](https://doi.org/10.1257/jel.20221319)
- 143 [6] Joseph Aylett-Bullock, Carolina Cuesta-Lazaro, Arnau Quera-Bofarull, Miguel Icaza-Lizaola,  
144 Aidan Sedgewick, Henry Truong, Aoife Curran, Edward Elliott, Tristan Caulfield, Kevin Fong,  
145 Ian Vernon, Julian Williams, Richard Bower, and Frank Krauss. 2021. June: Open-Source  
146 Individual-Based Epidemiology Simulation. *Royal Society Open Science* 8, 7 (July 2021),  
147 210506. <https://doi.org/10.1098/rsos.210506>
- 148 [7] Atilim Gunes Baydin, Barak A. Pearlmutter, Alexey Andreyevich Radul, and Jeffrey Mark  
149 Siskind. 2018. Automatic Differentiation in Machine Learning: A Survey. *Journal of Machine*  
150 *Learning Research* 18, 153 (2018), 1–43.
- 151 [8] Donald Beaver. 1992. Efficient Multiparty Protocols Using Circuit Randomization. In *Advances*  
152 *in Cryptology—CRYPTO'91: Proceedings 11*. Springer, 420–432.
- 153 [9] Claudio Bettini, Sergio Mascetti, X Sean Wang, Dario Freni, and Sushil Jajodia. 2009.  
154 Anonymity and Historical-Anonymity in Location-Based Services. *Privacy in location-based*  
155 *applications: research issues and emerging trends* (2009), 1–30.
- 156 [10] Parantapa Bhattacharya, Jiangzhuo Chen, Stefan Hoops, Dustin Machi, Bryan Lewis, Srinivasan  
157 Venkatramanan, Mandy L Wilson, Brian Klahn, Aniruddha Adiga, Benjamin Hurt, et al. 2023.  
158 Data-Driven Scalable Pipeline Using National Agent-Based Models for Real-Time Pandemic  
159 Response and Decision Support. *The International Journal of High Performance Computing*  
160 *Applications* 37, 1 (2023), 4–27.
- 161 [11] Keith R. Bisset, Jiangzhuo Chen, Xizhou Feng, V.S. Anil Kumar, and Madhav V. Marathe.  
162 2009. EpiFast: A Fast Algorithm for Large Scale Realistic Epidemic Simulations on Distributed  
163 Memory Systems. In *Proceedings of the 23rd International Conference on Supercomputing*  
164 *(ICS '09)*. Association for Computing Machinery, New York, NY, USA, 430–439. <https://doi.org/10.1145/1542275.1542336>  
165
- 166 [12] Eric Bonabeau. 2002. Agent-Based Modeling: Methods and Techniques for Simulating Human  
167 Systems. *Proceedings of the National Academy of Sciences of the United States of America* 99,  
168 10 (2002), 7280–7287. *arXiv:3057854*
- 169 [13] Stanislav S. Borysov, Jeppe Rich, and Francisco C. Pereira. 2019. How to Generate Micro-  
170 Agents? A Deep Generative Modeling Approach to Population Synthesis. *Transportation*  
171 *Research Part C: Emerging Technologies* 106 (Sept. 2019), 73–97. [https://doi.org/10.](https://doi.org/10.1016/j.trc.2019.07.006)  
172 [1016/j.trc.2019.07.006](https://doi.org/10.1016/j.trc.2019.07.006)
- 173 [14] US Census Bureau. [n.d.]. Why the Census Bureau Chose Differential Privacy.  
174 <https://www.census.gov/library/publications/2023/decennial/c2020br-03.html>.
- 175 [15] Kevin Chapuis, Patrick Taillandier, and Alexis Drogoul. 2022. Generation of Synthetic Popula-  
176 tions in Social Simulations: A Review of Methods and Practices. *Journal of Artificial Societies*  
177 *and Social Simulation* 25, 2 (2022), 6.

- 178 [16] Badr-Eddine Cherief-Abdellatif and Pierre Alquier. 2020. MMD-Bayes: Robust Bayesian Esti-  
179 mation via Maximum Mean Discrepancy. In *Proceedings of The 2nd Symposium on Advances*  
180 *in Approximate Bayesian Inference*. PMLR, 1–21.
- 181 [17] Ayush Chopra. 2022. *Decision Making for Populations*. Ph.D. Dissertation. Massachusetts  
182 Institute of Technology.
- 183 [18] Ayush Chopra, Ramesh Raskar, Jayakumar Subramanian, Balaji Krishnamurthy, Esmā S Gel,  
184 Santiago Romero-Brufau, Kalyan S Pasupathy, and Thomas C Kingsley. 2021. DeepABM:  
185 Scalable and Efficient Agent-Based Simulations via Geometric Learning Frameworks—a Case  
186 Study for COVID-19 Spread and Interventions. In *2021 Winter Simulation Conference (WSC)*.  
187 IEEE, 1–12.
- 188 [19] Ayush Chopra, Alexander Rodríguez, Jayakumar Subramanian, Arnau Quera-Bofarull, Balaji  
189 Krishnamurthy, B. Aditya Prakash, and Ramesh Raskar. 2023. Differentiable Agent-based  
190 Epidemiology. In *Proceedings of the 2023 International Conference on Autonomous Agents*  
191 *and Multiagent Systems (AAMAS '23)*. International Foundation for Autonomous Agents and  
192 Multiagent Systems, Richland, SC, 1848–1857.
- 193 [20] Abdoul-Ahad Choupani and Amir Reza Mamdoohi. 2016. Population Synthesis Using Iterative  
194 Proportional Fitting (IPF): A Review and Future Research. *Transportation Research Procedia*  
195 17 (Jan. 2016), 223–233. <https://doi.org/10.1016/j.trpro.2016.11.078>
- 196 [21] Joseph Cox. 2019. T-Mobile ‘Put My Life in Danger’ Says Woman Stalked With Black Market  
197 Location Data.
- 198 [22] Peter Sheridan Dodds and Duncan J. Watts. 2004. Universal Behavior in a Generalized Model  
199 of Contagion. *Physical Review Letters* 92, 21 (May 2004), 218701. [https://doi.org/10.](https://doi.org/10.1103/PhysRevLett.92.218701)  
200 [1103/PhysRevLett.92.218701](https://doi.org/10.1103/PhysRevLett.92.218701)
- 201 [23] Joel Dyer, Patrick Cannon, J. Doyne Farmer, and Sebastian Schmon. 2022. Black-Box Bayesian  
202 Inference for Economic Agent-Based Models. [https://doi.org/10.48550/arXiv.2202.](https://doi.org/10.48550/arXiv.2202.00625)  
203 [00625 arXiv:2202.00625 \[cs, econ, stat\]](https://doi.org/10.48550/arXiv.2202.00625)
- 204 [24] Wouter Edeling, Hamid Arabnejad, Robbie Sinclair, Diana Suleimenova, Krishnakumar  
205 Gopalakrishnan, Bartosz Bosak, Derek Groen, Imran Mahmood, Daan Crommelin, and  
206 Peter V. Coveney. 2021. The Impact of Uncertainty on Predictions of the CovidSim Epi-  
207 demiological Code. *Nature Computational Science* 1, 2 (Feb. 2021), 128–135. [https:](https://doi.org/10.1038/s43588-021-00028-9)  
208 [//doi.org/10.1038/s43588-021-00028-9](https://doi.org/10.1038/s43588-021-00028-9)
- 209 [25] Enrique Frias-Martinez, Graham Williamson, and Vanessa Frias-Martinez. 2011. An Agent-  
210 Based Model of Epidemic Spread Using Human Mobility and Social Network Information. In  
211 *2011 IEEE Third International Conference on Privacy, Security, Risk and Trust and 2011 IEEE*  
212 *Third International Conference on Social Computing*. IEEE, 57–64.
- 213 [26] Oded Goldreich, Silvio Micali, and Avi Wigderson. 2019. How to Play Any Mental Game, or a  
214 Completeness Theorem for Protocols with Honest Majority. In *Providing Sound Foundations*  
215 *for Cryptography: On the Work of Shafi Goldwasser and Silvio Micali*. 307–328.
- 216 [27] Chang Gong, Oleg Milberg, Bing Wang, Paolo Vicini, Rajesh Narwal, Lorin Roskos, and  
217 Aleksander S. Popel. 2017. A Computational Multiscale Agent-Based Model for Simulating  
218 Spatio-Temporal Tumour Immune Response to PD1 and PDL1 Inhibition. *Journal of The Royal*  
219 *Society Interface* 14, 134 (Sept. 2017), 20170320. [https://doi.org/10.1098/rsif.2017.](https://doi.org/10.1098/rsif.2017.0320)  
220 [0320](https://doi.org/10.1098/rsif.2017.0320)
- 221 [28] Gov.uk. [n.d.]. List of Ethnic Groups. [https://www.ethnicity-facts-figures.service.gov.uk/style-](https://www.ethnicity-facts-figures.service.gov.uk/style-guide/ethnic-groups)  
222 [guide/ethnic-groups](https://www.ethnicity-facts-figures.service.gov.uk/style-guide/ethnic-groups).
- 223 [29] Jakob Grazzini, Matteo G. Richiardi, and Mike Tsionas. 2017. Bayesian Estimation of Agent-  
224 Based Models. *Journal of Economic Dynamics and Control* 77 (April 2017), 26–47. [https:](https://doi.org/10.1016/j.jedc.2017.01.014)  
225 [//doi.org/10.1016/j.jedc.2017.01.014](https://doi.org/10.1016/j.jedc.2017.01.014)

- 226 [30] Daniel Günther, Marco Holz, Benjamin Judkewitz, Helen Möllering, Benny Pinkas, Thomas  
227 Schneider, and Ajith Suresh. 2022. Privacy-Preserving Epidemiological Modeling on Mobile  
228 Graphs. arXiv:2206.00539 [cs]
- 229 [31] Carmit Hazay and Yehuda Lindell. 2010. A Note on the Relation between the Definitions of  
230 Security for Semi-Honest and Malicious Adversaries. *Cryptology ePrint Archive* (2010).
- 231 [32] Robert Hinch, William J. M. Probert, Anel Nurtay, Michelle Kendall, Chris Wymant, Matthew  
232 Hall, Katrina Lythgoe, Ana Bulas Cruz, Lele Zhao, Andrea Stewart, Luca Ferretti, Daniel  
233 Montero, James Warren, Nicole Mather, Matthew Abueg, Neo Wu, Olivier Legat, Katie Bent-  
234 ley, Thomas Mead, Kelvin Van-Vuuren, Dylan Feldner-Busztin, Tommaso Ristori, Anthony  
235 Finkelstein, David G. Bonsall, Lucie Abeler-Dörner, and Christophe Fraser. 2021. OpenABM-  
236 Covid19—An Agent-Based Model for Non-Pharmaceutical Interventions against COVID-  
237 19 Including Contact Tracing. *PLOS Computational Biology* 17, 7 (July 2021), e1009146.  
238 <https://doi.org/10.1371/journal.pcbi.1009146>
- 239 [33] John H. Holland and John H. Miller. 1991. Artificial Adaptive Agents in Economic Theory.  
240 *The American Economic Review* 81, 2 (1991), 365–370. arXiv:2006886
- 241 [34] Bennett Cyphers and Jason Kelley. 2021. Illinois Bought Invasive Phone Location Data From  
242 Banned Broker Safegraph. [https://www.eff.org/deeplinks/2021/08/illinois-bought-invasive-  
243 phone-location-data-banned-broker-safegraph](https://www.eff.org/deeplinks/2021/08/illinois-bought-invasive-phone-location-data-banned-broker-safegraph).
- 244 [35] Cliff C. Kerr, Robyn M. Stuart, Dina Mistry, Romesh G. Abeysuriya, Katherine Rosenfeld,  
245 Gregory R. Hart, Rafael C. Núñez, Jamie A. Cohen, Prashanth Selvaraj, Brittany Hagedorn,  
246 Lauren George, Michał Jastrzębski, Amanda S. Izzo, Greer Fowler, Anna Palmer, Dominic  
247 Delport, Nick Scott, Sherrie L. Kelly, Caroline S. Bennette, Bradley G. Wagner, Stewart T.  
248 Chang, Assaf P. Oron, Edward A. Wenger, Jasmina Panovska-Griffiths, Michael Famulare,  
249 and Daniel J. Klein. 2021. Covasim: An Agent-Based Model of COVID-19 Dynamics and  
250 Interventions. *PLOS Computational Biology* 17, 7 (July 2021), e1009149. [https://doi.  
251 org/10.1371/journal.pcbi.1009149](https://doi.org/10.1371/journal.pcbi.1009149)
- 252 [36] Kamlesh Khunti, Awadhesh Kumar Singh, Manish Pareek, and Wasim Hanif. 2020. Is Ethnicity  
253 Linked to Incidence or Outcomes of Covid-19? *BMJ* 369 (April 2020), m1548. [https:  
254 //doi.org/10.1136/bmj.m1548](https://doi.org/10.1136/bmj.m1548)
- 255 [37] Jeremias Knoblauch, Jack Jewson, and Theodoros Damoulas. 2022. An Optimization-Centric  
256 View on Bayes’ Rule: Reviewing and Generalizing Variational Inference. *The Journal of*  
257 *Machine Learning Research* 23, 1 (2022), 5789–5897.
- 258 [38] Yehuda Lindell. 2020. Secure Multiparty Computation (MPC). *Cryptology ePrint Archive*  
259 (2020).
- 260 [39] Ilya Loshchilov and Frank Hutter. 2019. Decoupled Weight Decay Regularization. In *Internat-  
261 ional Conference on Learning Representations*.
- 262 [40] Yanir Marmor, Alex Abbey, Yuval Shahar, and Osnat Mokryn. 2023. Assessing Individual  
263 Risk and the Latent Transmission of COVID-19 in a Population with an Interaction-Driven  
264 Temporal Model. *Scientific Reports* 13, 1 (Aug. 2023), 12955. [https://doi.org/10.1038/  
265 s41598-023-39817-9](https://doi.org/10.1038/s41598-023-39817-9)
- 266 [41] Christopher A. Martin, David R. Jenkins, Jatinder S. Minhas, Laura J. Gray, Julian Tang,  
267 Caroline Williams, Shirley Sze, Daniel Pan, William Jones, Raman Verma, Scott Knapp,  
268 Rupert Major, Melanie Davies, Nigel Brunskill, Martin Wiselka, Chris Brightling, Kamlesh  
269 Khunti, Pranab Haldar, and Manish Pareek. 2020. Socio-Demographic Heterogeneity in the  
270 Prevalence of COVID-19 during Lockdown Is Associated with Ethnicity and Household Size:  
271 Results from an Observational Cohort Study. *eClinicalMedicine* 25 (Aug. 2020). [https:  
272 //doi.org/10.1016/j.eclinm.2020.100466](https://doi.org/10.1016/j.eclinm.2020.100466)
- 273 [42] Derek Meyer and George G. Vega Yon. 2023. epiworldR: Fast Agent-Based Epi Models.  
274 *Journal of Open Source Software* 8, 90 (Oct. 2023), 5781. [https://doi.org/10.21105/  
275 joss.05781](https://doi.org/10.21105/joss.05781)

- 276 [43] Shakir Mohamed, Mihaela Rosca, Michael Figurnov, and Andriy Mnih. 2020. Monte Carlo  
277 Gradient Estimation in Machine Learning. *Journal of Machine Learning Research* 21, 132  
278 (2020), 1–62.
- 279 [44] Alexander Mordvintsev, Ettore Randazzo, and Craig Fouts. 2022. Growing Isotropic Neural Cel-  
280 lular Automata. <https://doi.org/10.48550/arXiv.2205.01681> arXiv:2205.01681 [cs,  
281 q-bio]
- 282 [45] Kirill Müller and Kay W. Axhausen. 2010. Population Synthesis for Microsimulation: State of  
283 the Art. *Arbeitsberichte Verkehrs- und Raumplanung* 638 (Aug. 2010). [https://doi.org/  
284 10.3929/ethz-a-006127782](https://doi.org/10.3929/ethz-a-006127782)
- 285 [46] Marco Pangallo, Alberto Aleta, R. Maria del Rio Chanona, Anton Pichler, David Martín-Corral,  
286 Matteo Chinazzi, François Lafond, Marco Ajelli, Esteban Moro, Yamir Moreno, Alessandro  
287 Vespignani, and J. Doyne Farmer. 2022. The Unequal Effects of the Health-Economy Trade-  
288 off during the COVID-19 Pandemic. <https://doi.org/10.48550/arXiv.2212.03567>  
289 arXiv:2212.03567 [physics, q-fin]
- 290 [47] Donovan Platt. 2020. A Comparison of Economic Agent-Based Model Calibration Methods.  
291 *Journal of Economic Dynamics and Control* 113 (April 2020), 103859. [https://doi.org/  
292 10.1016/j.jedc.2020.103859](https://doi.org/10.1016/j.jedc.2020.103859)
- 293 [48] Arnau Quera-Bofarull, Ayush Chopra, Joseph Aylett-Bullock, Carolina Cuesta-Lazaro, Anisoara  
294 Calinescu, Ramesh Raskar, and Michael Wooldridge. 2023. Don’t Simulate Twice: One-shot  
295 Sensitivity Analyses via Automatic Differentiation. In *Proceedings of the 2023 International  
296 Conference on Autonomous Agents and Multiagent Systems (AAMAS ’23)*. International Founda-  
297 tion for Autonomous Agents and Multiagent Systems, Richland, SC, 1867–1876.
- 298 [49] Arnau Quera-Bofarull, Ayush Chopra, Anisoara Calinescu, Michael Wooldridge, and Joel  
299 Dyer. 2023. Bayesian Calibration of Differentiable Agent-Based Models. *arXiv preprint  
300 arXiv:2305.15340* (2023). arXiv:2305.15340
- 301 [50] Arnau Quera-Bofarull, Joel Dyer, Anisoara Calinescu, J. Doyne Farmer, and Michael  
302 Wooldridge. 2023. BlackBIRDS: Black-Box Inference foR Differentiable Simulators. *Journal of  
303 Open Source Software* 8, 89 (Sept. 2023), 5776. <https://doi.org/10.21105/joss.05776>
- 304 [51] Arnau Quera-Bofarull, Joel Dyer, Anisoara Calinescu, and Michael Wooldridge. 2023. Some  
305 Challenges of Calibrating Differentiable Agent-Based Models. [https://doi.org/10.  
306 48550/arXiv.2307.01085](https://doi.org/10.48550/arXiv.2307.01085) arXiv:2307.01085 [cs, q-fin, stat]
- 307 [52] Santiago Romero-Brufau, Ayush Chopra, Alex J Ryu, Esmá Gel, Ramesh Raskar, Walter  
308 Kremers, Karen S Anderson, Jayakumar Subramanian, Balaji Krishnamurthy, Abhishek Singh,  
309 et al. 2021. Public Health Impact of Delaying Second Dose of BNT162b2 or mRNA-1273  
310 Covid-19 Vaccine: Simulation Agent Based Modeling Study. *BMJ (Clinical research ed.)* 373  
311 (2021).
- 312 [53] Ludger Ruschendorf. 1995. Convergence of the Iterative Proportional Fitting Procedure. *The  
313 Annals of Statistics* 23, 4 (1995), 1160–1174. arXiv:2242759
- 314 [54] Vincent Stimper, David Liu, Andrew Campbell, Vincent Berenz, Lukas Ryll, Bernhard  
315 Schölkopf, and José Miguel Hernández-Lobato. 2023. Normflows: A PyTorch Package  
316 for Normalizing Flows. *Journal of Open Source Software* 8, 86 (2023), 5361. [https:  
317 //doi.org/10.21105/joss.05361](https://doi.org/10.21105/joss.05361)
- 318 [55] Guus ten Broeke, George van Voorn, and Arend Ligtenberg. 2016. Which Sensitivity Analysis  
319 Method Should I Use for My Agent-Based Model? *Journal of Artificial Societies and Social  
320 Simulation* 19, 1 (2016), 5.
- 321 [56] Zhibo Wang, Xiaoyi Pang, Yahong Chen, Huajie Shao, Qian Wang, Libing Wu, Honglong Chen,  
322 and Hairong Qi. 2018. Privacy-Preserving Crowd-Sourced Statistical Data Publishing with an  
323 Untrusted Server. *IEEE Transactions on Mobile Computing* 18, 6 (2018), 1356–1367.
- 324 [57] Andrew C Yao. 1982. Protocols for Secure Computations. In *23rd Annual Symposium on  
325 Foundations of Computer Science (Sfcs 1982)*. IEEE, 160–164.

326 [58] Shuli Zhou, Suhong Zhou, Zhong Zheng, and Junwen Lu. 2021. Optimizing Spatial Allocation  
 327 of COVID-19 Vaccine by Agent-Based Spatiotemporal Simulations. *GeoHealth* 5, 6 (2021),  
 328 e2021GH000427. <https://doi.org/10.1029/2021GH000427>

## 329 6 Appendix

### 330 6.1 The GMW protocol

331 The GMW protocol uses additive secret sharing to communicate (or aggregate) private inputs across  
 332 the participant entities. The key insight is to divide a secret input into multiple shares in such a way  
 333 that the secret can be reconstructed only when a sufficient number of shares are combined together.  
 334 The scheme supports diverse aggregation queries such as secure addition, or secure multiplication [8]  
 335 of the secrets held by the participating agents. Here we focus on the addition case and we assume  
 336 that all participating agents are required to compute the secret, usually denoted by  $t = N$ , but the  
 337 same methodology can be extended to multiplication and composite queries (see, e.g., [38]).

338 Consider  $N$  agents holding private values  $s_i$ . We want to compute the sum  $\sum_i s_i$  without any  
 339 agent  $j$  acquiring knowledge about  $s_{\{k \neq j\}}$ . To setup the protocol, the agents agree an integer  
 340  $n > \max\{s_1, \dots, s_N\}$  defining the finite group  $\mathbb{Z}_n$  on which all computations will be carried <sup>1</sup>. Each  
 341 agent  $i$  then samples  $N - 1$  random numbers,  $r_{ij} \sim \mathcal{U}\{0, n - 1\}$ , such that the input is divided into  
 342  $N$  shares,  $s_{ij}$  defined by

$$s_i = \sum_{j=1}^N s_{ij} \pmod{n} = \sum_{j=1}^{N-1} r_{ij} + \left( s_i - \sum_{j=1}^{N-1} r_{ij} \right) \pmod{n}. \quad (2)$$

343 Each agent then sends each share of their secret to each corresponding agent; agent  $i$  sends  $s_{i1}$  share  
 344 to agent 1,  $s_{i2}$  share to agent 2, etc. Locally, each agent performs the sum

$$\sigma_k = \sum_{i=1}^N s_{ik} \pmod{n}. \quad (3)$$

345 Finally, all values  $\sigma_k$  are shared so that the reconstructed sum,  $S = \sum_k \sigma_k \pmod{n}$ , can be computed  
 346 which corresponds to the sum of the agent inputs  $s_i$  by construction. Typically, this reconstruction  
 347 may be conducted by a central MPC server or a trusted agent. We summarize the protocol in  
 348 Algorithm 1 and we provide an illustrating example below.

#### 349 6.1.1 Additive secret sharing example

350 Consider  $N = 3$  agents—Alice, Bob, and Carol— holding private values  $s_A = 2$ ,  $s_B = 3$ , and  
 351  $s_C = 5$ . They wish to compute the sum of these values without disclosing their individual inputs.  
 352 They agree on an integer  $n = 11$ , defining a finite group  $\mathbb{Z}_n$ . First, the agents generate 3 shares each,  
 353 by sampling 2 random numbers from  $\mathbb{Z}_n$ . For instance, Alice generates random numbers 7 and 5, so  
 354 that

$$s_A = s_{AA} + s_{AB} + s_{AC} = 7 + 5 + 1 \pmod{11} = 2, \quad (4)$$

355 and similarly for Bob and Carol with  $s_B = 2 + 0 + 1 \pmod{11}$ , and  $s_C = 3 + 1 + 1 \pmod{11}$ .  
 356 Second, the agents communicate with each other to keep one of the shares and send the other two to  
 357 the other two agents and perform the sum of the received shares. For example, Alice receives  $s_{BA}$   
 358 from Bob and  $s_{CA}$  from Carol and computes

$$\sigma_A = s_{AA} + s_{BA} + s_{CA} = 7 + 2 + 3 \pmod{11} = 1 \pmod{11}, \quad (5)$$

359 and similarly for Bob and Carol with  $\sigma_B = 5 + 0 + 1 \pmod{11} = 6 \pmod{11}$  and  $\sigma_C =$   
 360  $1 + 1 + 1 \pmod{11} = 3 \pmod{11}$ . Finally, the secret can be reconstructed by doing  $S =$   
 361  $\sigma_A + \sigma_B + \sigma_C = 10 \pmod{11}$  as expected.

362 In the following section, we apply the GMW protocol to generalize the above insight to share  
 363 information containing agent’s private information to other agents or a central MPC server, providing  
 364 protocols for the computation of agent updates (Equation (1)), and gradients in a secure way, enabling  
 365 privacy-preserving simulation, calibration, and analysis of ABMs.

<sup>1</sup>The choice to perform finite group arithmetics is so that no information about the secret can be gained by holding  $< N$  shares.

## 366 7 Case Study: Privacy-preserving Epidemiology

367 In this section, we aim to illustrate a practical example where this new ABM methodology could be  
 368 deployed, by showing a simulation and calibration of a decentralized, privacy-preserving, agent-based  
 369 SIR model.

370 The model follows a standard parameterization where agents' interactions are specified through  
 371 a contact graph  $\mathcal{G}$ , which in this case is only locally defined by each agent having access to their  
 372 neighbors. Each agent has 3 possible states, 0 (Susceptible), 1 (Infected), and 2 (Recovered). We  
 373 initialize the simulation by infecting a fraction  $I_0$  of agents, which are sampled uniformly from the  
 374 population, while the remaining agents are considered to be susceptible. Following the notation  
 375 introduced in Section 2, at each time-step, agent  $i$  updates its state following Equation (1) with

$$M_{ij}(t) = I_j(t) \quad (6)$$

376 where  $I_j(t)$  is the infected status of the neighbor (0 or 1), so that

$$\begin{aligned} z_i(t+1) = & \mathbb{1}_{\{z_i=0\}} \cdot \text{Bernoulli}\left(p_{\text{inf}}^{(i)}(t)\right) + \\ & \mathbb{1}_{\{z_i=1\}} \cdot \left(1 + \text{Bernoulli}\left(p_{\text{rec}}^{(i)}\right)\right) + \\ & \mathbb{1}_{\{z_i=2\}} \cdot 2 \end{aligned} \quad (7)$$

377 with

$$p_{\text{inf}}^{(i)}(t) = 1 - \exp\left(-\frac{\beta S_i \Delta t}{n_i} \sum_{j \in \mathcal{N}(i)} I_j(t)\right), \quad (8)$$

378 where  $\mathcal{N}(i)$  is the set of neighbors of agent  $i$ ,  $S_i$  is the susceptibility of agent  $i$ ,  $n_i = \#\mathcal{N}(i)$  is the  
 379 total number of neighbors,  $\Delta t$  is the duration of the time-step, and  $\beta$  is a structural parameter of the  
 380 ABM called the effective contact rate. Infected agents can recover at each time-step with recovery  
 381 rate  $\gamma$ , so that

$$p_{\text{rec}}^{(i)} = 1 - \exp(-\gamma \Delta t). \quad (9)$$

382 For the case of a complete graph, the model reduces to the standard ODE-based SIR model with  
 383  $R_0 = \beta/\gamma$  as the basic reproduction number. The model is run for  $n_t$  time-steps.

384 To ground the example on real data, we consider the contact graph of the city of XXX, extracted from  
 385 the June ABM model [6] to determine the neighborhood of each agent,  $\mathcal{N}(i)$ . This contact graph  
 386 includes the interactions of agents in households, companies, and schools and it is based on English  
 387 census data. The choice of parameter values for the experiment is given in Table 1.

Parameter	Value
$\beta$	$0.5 \text{ day}^{-1}$
$\gamma$	$0.1 \text{ day}^{-1}$
$I_0$	0.01
$\Delta t$	1 day
$n_t$	60
$\mathcal{G}$	XXX

Table 1: Parameter values for the considered agent-based SIR model.

### 388 7.1 Private policy assessment with ABMs

389 We first consider the application of the SECURESIMULATION protocol (Algorithm 3). Let us pose a  
 390 situation where a policy maker wants to study the efficacy of mask-wearing at different compliance  
 391 levels using agent-based simulation. We introduce a slight modification to Equation (8) to incorporate  
 392 a reduction on the infection probability due to mask-wearing with certain compliance  $\alpha$ ,

$$p_{\text{inf}}^{(i)}(t) = 1 - \exp\left(-\frac{\beta S_i \Delta t}{n_i} \sum_{j \in \mathcal{N}(i)} I_j(t)(1 - c_j)\right), \quad (10)$$

393 where  $c_j \sim \text{Bernoulli}(\alpha)$ , so that  $\alpha_i = 1$  corresponds to full compliance where there is no trans-  
 394 mission. Note that we are assuming, complete protection against infection when wearing a mask.  
 395 We proceed to execute 3 simulations for 3 different values of  $\alpha$ . At each simulation,  $\alpha$  is sent to the  
 396 agents, where they locally compute their own compliance to the measure. The SecureSimulation  
 397 protocol is then used to run the simulation and retrieve the aggregate statistic of interest,  $\mathbf{x}$ , which in  
 398 this case is the number of infections over time. The results are shown in Figure 2, where we observe  
 399 that little transmission occurs when compliance is above 75%.

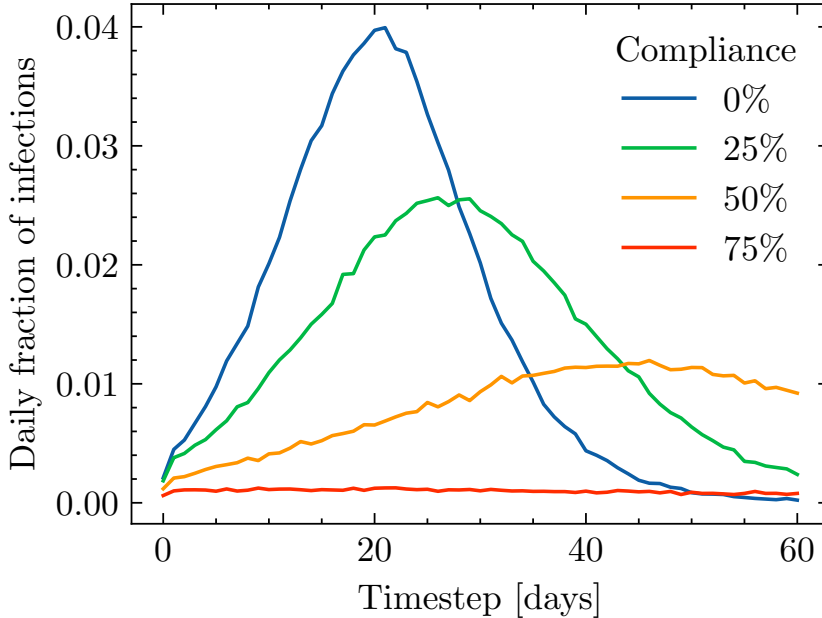


Figure 2: Infection curves for different levels of compliance: 0% (blue), 25% (green), 50% (orange), 75% (red). The number of infections has been normalized to the number of agents  $N$ .

400 Thus we observe that within our privacy-preserving methodology, the policy maker could still have  
 401 access to the same level of insight than a traditional ABM, all while protecting the individual agent’s  
 402 privacy.

## 403 7.2 Private calibration of ABMs

404 Next, we pose a situation where we want to calibrate our ABM with structural parameters  $\theta = (\beta, \gamma)$   
 405 to observed ground-truth data. For simplicity, we present the calibration of the  $\beta$  parameter given an  
 406 observed curve of infections ( $\mathbf{y}$ ), obtained by running the ABM model with the baseline parameters  
 407 in Table 1.

408 The first step is to compute the gradient  $\nabla_{\theta} \mathbf{x}$ , where  $\mathbf{x}$  is the number of daily infections and  $\theta = \beta$ .  
 409 We note that this gradient can be approximated by the gradient of the average number of new  
 410 infections with respect to  $\beta$ ,

$$\frac{\partial x_t}{\partial \beta} \approx \frac{\partial \mathbb{E}[\Delta I(t)]}{\partial \beta} = \sum_{i=1}^N \chi_i(t) \exp(-\chi_i(t)/\beta), \quad (11)$$

411 where

$$\chi_i(t) = \exp\left(-\frac{\beta S_i \Delta t}{n_i} \sum_{j \in \mathcal{N}(i)} I_j(t)\right). \quad (12)$$

412 The gradient can be safely retrieved by a central agent by performing the SECRETSHARING protocol  
 413 across all agents as described in Algorithm 3. We thus conduct GVI by considering  $Q$  to be a  
 414 masked-autoregressive normalizing flow, and assume the prior is a normal distribution with  $\mu = 0.7$   
 415 and  $\sigma = 0.5$ .

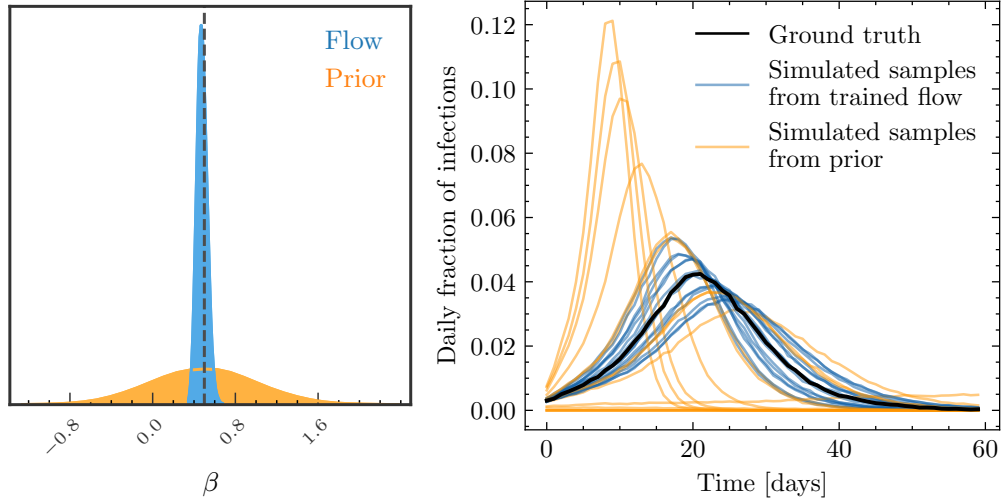


Figure 3: Left: Probability density plot for the trained normalizing flow (blue) against the prior distribution (orange). Ground-truth value is marked as a dashed black line. Right: Results from simulating  $\beta$  samples from the trained flow (blue) and prior (orange) compared to the ground-truth data (black). The number of infections has been normalized to the number of agents  $N$ .

416 Figure 3 (left) shows the trained normalizing flow which correctly assigns high probability mass to  
 417 the ground-truth value. To further evaluate the goodness of the fit, we plot simulated runs from ABM  
 418 parameters sampled from the trained flow in Figure 3 (right), where we compare it to runs simulated  
 419 from prior samples.

420 This experiment highlights how privacy-preserving ABM can be integrated into probabilistic pro-  
 421 gramming pipelines, like the considered case where we have used the Bayesian gradient-assisted  
 422 inference algorithms in the BLACKBIRDS software package. This opens the door into integrating  
 423 ABM insight into more complex ML pipelines leveraging heterogeneous data streams to boost the  
 424 model’s insight capabilities.